The dynamic role of genetics on cortical patterning during childhood and adolescence

J. Eric Schmitt[a,1], Michael C. Neale[b], Bilqis Fassassi[c], Javier Perez[b], Rhoshel K. Lenroot[d], Elizabeth M. Wells[c], and Jay N. Giedd[c]

[a]Department of Radiology, Hospital of the University of Pennsylvania, Philadelphia, PA 19104; [b]Department of Psychiatry, Virginia Institute for Psychiatric and Behavioral Genetics, Virginia Commonwealth University, Richmond, VA 23298-980126; [c]Pediatric Imaging Unit, National Institutes of Mental Health, Bethesda, MD 20892; and [d]School of Psychiatry and Neuroscience Research Australia, University of New South Wales, Sydney, 2052, Australia

Edited by Marcus E. Raichle, Washington University, St. Louis, MO, and approved March 25, 2014 (received for review June 19, 2013)

Longitudinal imaging and quantitative genetic studies have both provided important insights into the nature of human brain development. In the present study we combine these modalities to obtain dynamic anatomical maps of the genetic contributions to cortical thickness through childhood and adolescence. A total of 1,748 anatomic MRI scans from 792 healthy twins and siblings were studied with up to eight time points per subject. Using genetically informative latent growth curve modeling of 81,924 measures of cortical thickness, changes in the genetic contributions to cortical development could be visualized across the age range at high resolution. There was highly statistically significant ($P < 0.0001$) genetic variance throughout the majority of the cerebral cortex, with the regions of highest heritability including the most evolutionarily novel regions of the brain. Dynamic modeling of changes in heritability over time demonstrated that the heritability of cortical thickness increases gradually throughout late childhood and adolescence, with sequential emergence of three large regions of high heritability in the temporal poles, the inferior parietal lobes, and the superior and dorsolateral frontal cortices.

neurodevelopment | twin research

Individual differences in brain structure and function provide the biological substrate for population-level variation in cognition and behavior. By characterizing patterns of variance and covariance in brain endophenotypes within families, statistical genetic studies have demonstrated that genetic factors are the dominant force in explaining variance in many measures of brain structure throughout the life cycle (1). For measures of cortical thickness in typically developing youth, the frontal lobe and language centers are among the most heritable, with global patterns of heritability resembling maps of cortical structures that are evolutionarily novel in humans relative to other primates (2).

In a separate thread of research, longitudinal in vivo studies of human brain development have demonstrated the extraordinarily dynamic nature of the cerebral cortex throughout childhood and adolescence. In general, primary sensory cortices mature before regions of the cerebral cortex more associated with higher cognitive functions (3). The rate of decrease in cortical thickness also varies widely throughout the brain, with the most rapidly changing regions including the bilateral superior parietal cortices and the right frontal lobe (4).

To date, genetically informative developmental imaging studies have been limited to either cross sectional data (2) or longitudinal studies with two time points (5). To quantify the genetic contributions to pediatric cortical maturation, we applied latent growth curve models to high-resolution measures of cortical thickness from a large genetically informative longitudinal sample acquired by the National Institutes of Mental Health. These analyses enabled the visualization of the genetic contributions to maturational timing through childhood and adolescence.

Results

The contribution of genetic factors to individual differences in cortical thickness was highly statistically significant and heterogeneous throughout the cerebrum (Fig. 1*A*). The regions with the most significant genetic variance were in the parietal lobes bilaterally, occipital poles, orbitofrontal cortex, frontal operculum superior temporal gyri, and left supramarginal gyrus. Dynamic models demonstrated that the heritability of cortical thickness increases gradually throughout late childhood and adolescence, with sequential emergence of three large regions of high heritability in the temporal poles, the inferior parietal lobe, and the superior and dorsolateral frontal cortices, respectively (Fig. 2, Fig. S1, and Movies S1–S4).

Although heritability represents the most commonly used statistic in quantitative genetics, its estimation depends on the total phenotypic variance. In other words, changes in total phenotypic variance can alter heritability, even if genetic effects are constant. Thus, we also examined the individual genetic and environmental variance components independently. These analyses identified statistically significant changes in genetic variance in the anterior frontal lobes, inferior parietal and parieto-occipital cortices, temporal poles, and the left inferior postcentral gyrus extending into the left supramarginal gyrus (Fig. 1*B*). There was striking asymmetry in genetic change in the frontal lobes, with most of the right anterior frontal lobe having significant effects but only the superior frontal gyrus and orbitofrontal gyrus in the left hemisphere. When modeled

Significance

Quantitative genetic studies have established that evolutionarily novel regions of the cerebral cortex have high heritability within human populations. Longitudinal imaging studies have demonstrated that the cerebral cortex is highly dynamic in childhood. In the current study, we examine how genetic effects on cortical thickness change longitudinally over childhood and adolescence using a large genetically informative imaging sample. We find rapid changes in genetic effects in early childhood, with stabilization in late adolescence. The areas with the greatest changes include evolutionarily novel regions. These findings have implications for future molecular genetic studies of imaging endophenotypes and further our sparse understanding of how genes help to shape the brain after birth.

Author contributions: J.E.S., M.C.N., R.K.L., E.M.W., and J.N.G. designed research; J.E.S., M.C.N., B.F., E.M.W., and J.N.G. performed research; J.E.S., J.P., and J.N.G. analyzed data; and J.E.S., M.C.N., J.P., R.K.L., and J.N.G. wrote the paper.

The authors declare no conflict of interest.

This article is a PNAS Direct Submission.

Freely available online through the PNAS open access option.

Data deposition: The data reported in this paper have been deposited in the Dryad repository, datadryad.org, doi:10.5061/dryad.5tp6r.

[1]To whom correspondence should be addressed. E-mail: eric.schmitt@stanfordalumni.org.

This article contains supporting information online at www.pnas.org/lookup/suppl/doi:10.1073/pnas.1311630111/-/DCSupplemental.

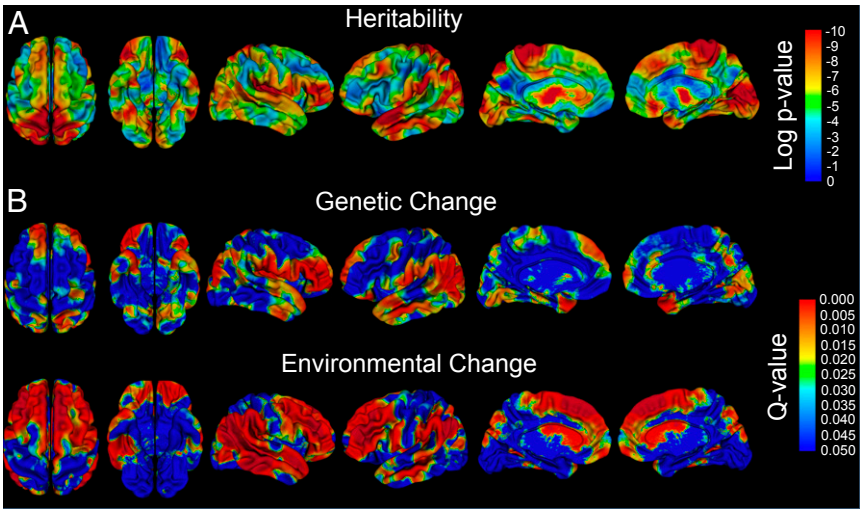

Fig. 1. Probability maps depicting regional differences in the significance of variance components. (*A*) A log transformed map of statistically significant genetic effects on individual differences in cortical thickness. All vertices were below a *q*-value threshold of 0.05 following correction for multiple testing. (*B*) Regions with statistically significant changes in variance components over childhood and adolescence.

dynamically, genetic variance was noted to *decrease* substantially over the age range, with a wave of decreasing genetic variance generally moving from posterior to anterior (Fig. 2 and Movie S5 and Movie S6). Toward the end of adolescence, there was relatively increased residual genetic variance in the anterior frontal lobe and anterior and superior temporal lobes.

Patterns of environmental change over time differed distinctly from their genetic counterparts, with the most significant regions of change in the dorsolateral prefrontal cortex (DLPFC) and the inferior parietal lobe (Figs. 1 and 2). Dynamic mapping of environmental variance demonstrated initial heterogeneity throughout the cerebrum, with highest variance in the frontal and parietal cortex. However, environmental variance in these regions decreases rapidly in early to middle childhood, with near-uniform, substantially diminished environmental variance by late childhood. Continued near-uniform decreases in variance were noted throughout adolescence.

We then reanalyzed the data allowing for sex differences in variance components. Sex-moderated models did not identify any significant differences between males and females after adjusting for multiple testing. The heritability patterns between males and females were slightly different, however. Sex differences in heritability increased in the frontal lobes, with males demonstrating higher heritability in late adolescence (Figs. S2 and S3). Males were noted to have higher heritability in the inferior temporal cortices in early childhood. A more complicated lateralized pattern was noted in the frontal operculum, with females demonstrating higher heritability on the left in early childhood and males higher on the right. Despite these subtle differences, cortical thickness heritability patterns were quite similar between the sexes.

Discussion

The present prospective longitudinal study confirms the highly dynamic nature of genetic variance in cortical thickness throughout the first two decades of life. The patterns of genetic change are regionally specific but generally proceed from posterior to anterior, similar to prior longitudinal phenotypic modeling of gray matter density (3) and cortical thickness (6). As in prior cross-sectional genetic studies, the regions of the highest heritability were primarily in association cortices and the frontal lobes, more evolutionarily novel regions of the brain (2). These combined findings are suggestive that many of the genes involved in evolution of the cerebral cortex are also involved in human developmental timing. Regional differences in heritability may be due to allelic fixation of evolutionarily older regions under selective pressure, with newer cortical regions still undergoing natural selection. Indeed, there is evidence that several genes involved in developmental abnormalities in brain volumes, most prominently the abnormal spindle-like microcephaly associated (ASPM) and microcephalin (MCPH1) genes, have undergone positive selection through recent primate evolution (7) and may still contribute to phenotypic variation within the typical human population (8, 9). Although the genes responsible for the dramatic developmental changes in human cortical thickness are unknown, genetic-variants involved in myelination (4) and synaptic pruning (10) are attractive potential biological targets.

The vast majority of genetically mediated changes in cortical thickness occurred in the first decade of life, with gross stability in genetic variance after age 12. Thus, the age of image acquisition is predicted to have a substantial effect on molecular genetic studies of brain endophenotypes. The temporal resolution of the existing molecular genetic studies on the human brain is limited, but the extant literature also is suggestive that genetic effects on brain structure are highly dynamic in childhood. For example, Colantuoni et al. (11) identified rapid decreases in the absolute rate of gene expression change in the prefrontal cortex during the first through third decades of life. A more comprehensive transriptome analysis by Kang et al. (12) on 15 developmental periods and 11 neocortical regions demonstrated dramatic changes in gene expression throughout childhood and adolescence, with sharp reductions in expression within the neocortex for numerous genes. The development of new informatics tools that fuse genetic and anatomic data such as the Allen brain atlas promise to further elucidate the complex spatiotemporal patterns of genetic expression within the human cerebral cortex (13).

In the current study, the regions of the brain with the most substantial changes in genetic variance strongly resemble those with the greatest annualized decreases in cortical thickness in a prior study by Sowell et al. (4) on 45 children scanned from ages 5–11 and suggest that genetic factors drive changes in these regions in early to middle childhood. In midchildhood, we observed stabilization of genetic contributions to individual differences in cortical thickness, with continued decreases in environmental variance. Similar findings were noted in a paper by van Soelen et al. (5) on a sample of 190 twins scanned at ages 9 and 12 y; the scan interval in that study is near the inflection point of the genetic

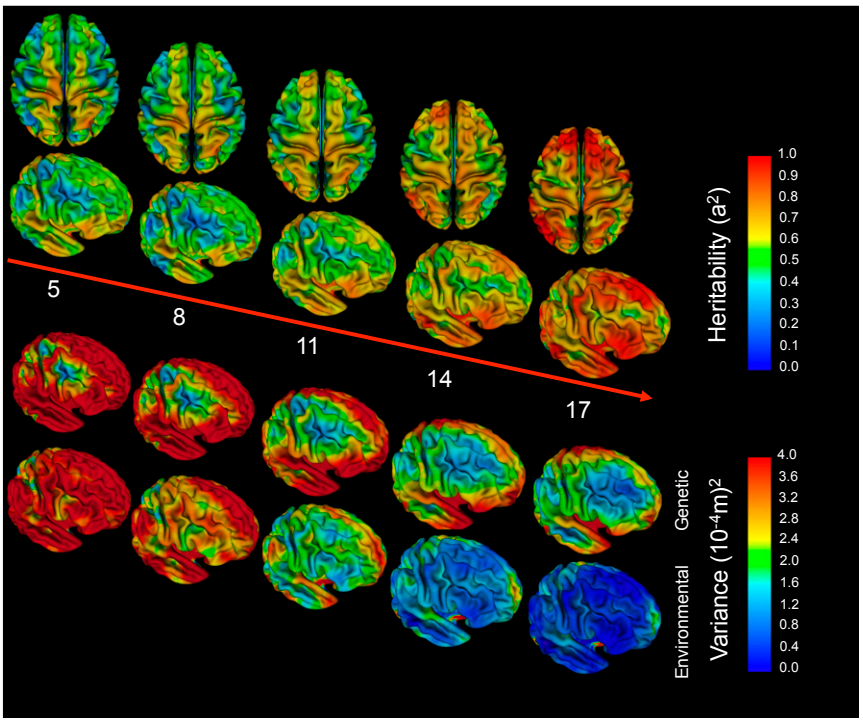

Fig. 2. Dynamic changes in the heritability of cortical thickness with age, also depicted in Movies S1–S6. (*Upper*) Superior and right lateral maps of heritability (the proportion of phenotypic variance attributable to genetic factors) for ages 5–17. (*Lower*) Right lateral views of changes in individual variance components with age.

variance trajectory observed in the present study. As in the current study, van Soelen et al. noted that progressive decreases in environmental variation were the predominant reason for changes in heritability over the age range that they studied.

Our exploratory analysis of gene × sex interactions suggested subtle differences in developmental timing of the frontal lobes and language centers bilaterally, including Broca's and Wernicke's areas. However, the findings from the current study did not reach statistical significance. Given evidence that females demonstrate disproportionate aptitude in verbal memory and verbal fluency (14), the localization of gene × sex interactions to these regions is consistent with the cognitive literature and warrants further investigation. However, prior phenotypic studies on the sexual dimorphism of cortical thickness are inconsistent, with many studies suggestive of no differences between sexes. In contrast, Luders et al. (15) identified significant sex differences in parieto-occipital cortex and the posterior superior frontal gyrus in unscaled data, with extensive sex differences noted after adjusting for global brain size. In a sample of 176 adults, Sowell et al. (16) demonstrated that females have relatively greater cortical thickness in the inferior parietal lobe, posterior temporal lobe, orbitofrontal cortex, and left frontal operculum. Other genetically informative imaging samples which include hormonal and pubertal data may be better positioned to directly test for sex effects (17).

In contrast to genetic variance, environmentally mediated variance in cortical thickness continues to decline throughout the second decade. The regions with the most dramatic changes in environmental variance include DLPFC and the supramarginal gyri bilaterally, regions implicated in the emergence of new cognitive and linguistic skills in late childhood and adolescence. Interestingly, these are the same regions with relatively increased gray matter density in adolescence (3). As environmental variance continues to decline and becomes near-uniform, genetic effects become the dominant explanatory factor in individual differences in cortical thickness, with heritability maps in late adolescence approaching those observed in adult populations (18).

Materials and Methods

Subjects. Seven-hundred and ninety-two normally developing children, adolescents, and young adults from 410 families were recruited as part of an ongoing longitudinal brain imaging project being conducted at the Child Psychiatry Branch of the National Institute of Mental Health (NIMH). The sample included pediatric, adolescent, and young adult monozygotic twins (MZ, $n = 249$), dizygotic twins (DZ, $n = 131$), siblings of twins ($n = 110$), and singleton ($n = 302$) family members (Table 1). Parents of prospective participants were interviewed by phone and asked to report their child's health, developmental, and educational history. During their visits to the NIMH, subjects underwent a clinical interview and physical examination. Subjects were excluded if they had taken psychiatric medications, had been diagnosed with a psychiatric disorder, had undergone brain trauma, or had any condition known to affect gross brain development. Inclusion criteria were a minimum gestational age of 29 wk and a minimum birth weight of 1,500 g.

Approximately 80% of families responding to the ads met inclusion criteria. Socioeconomic status was rated using the Hollingshead scale (19). For twin subjects, zygosity was determined by DNA analysis of buccal cheek swabs using 9–21 unlinked short tandem repeat loci for a minimum certainty of 99%, by BRT Laboratories and Proactive Genetics. We obtained verbal or written assent from the child and written consent from the parents for their participation in the study. The NIMH Institutional Review Board approved the protocol.

MRI Acquisition. All MRI images were acquired on the same General Electric 1.5 Tesla Signa Scanner located at the National Institutes of Health Clinical Center in Bethesda, MD. A 3D spoiled gradient recalled echo sequence in the steady state sequence was used to acquire 124 contiguous 1.5-mm thick slices in the axial plane (echo time/repetition time = 5/24 ms; flip angle = 45 degrees, matrix = 256 × 192, number of excitations = 1, field of view = 24 cm, acquisition time 9.9 min). A Fast Spin Echo/Proton Density weighted imaging sequence was also acquired for clinical evaluation. A total of 1,748 MRI datasets were acquired (Fig. 3). Up to eight MRI scans were performed per individual, with sibships containing up to five members. The mean interval between scans was 2.4 y.

Image Analysis. All MR images were imported into the CIVET pipeline for automated structural image processing (20). Briefly, the native MRI scans were registered into standardized stereotaxic space using a linear transformation (21) and corrected for nonuniformity artifacts (22). The registered and corrected volumes were segmented into white matter, gray matter,

Table 1. Demographic characteristics of the sample

	MZ	DZ	Siblings of twins	Singletons	Total
Sample size	249	131	110	302	792
Mean age at first scan, years (SD)	11.2 (3.8)	9.6 (3.5)	12.0 (4.4)	11.7 (5.1)	11.3 (4.4)
Mean scan interval, years (SD)	2.4 (0.66)	2.4 (0.67)	2.3 (0.86)	2.3 (0.85)	2.4 (1.1)
Sex					
Female	117 (47%)	62 (47%)	61 (55%)	136 (45%)	376 (47%)
Male	132 (53%)	69 (53%)	49 (45%)	166 (55%)	416 (53%)
SES, Hollingshead index (SD)	44.4 (18.6)	43.2 (15.1)	43.0 (18.0)	40.6 (20.3)	42.6 (18.7)
Handedness					
Right	215 (88%)	107 (82%)	88 (82%)	269 (90%)	679 (87%)
Mixed	16 (7%)	14 (11%)	7 (7%)	17 (6%)	54 (7%)
Left	14 (6%)	10 (8%)	12 (11%)	14 (5%)	50 (6%)

SES, socioeconomic status.

cerebrospinal fluid, and background using a neural net classifier (23). The gray and white matter surfaces were fitted using deformable surface-mesh models and nonlinearly aligned toward a template surface (24–26). The gray and white matter surfaces were resampled into native space, and cortical thickness was measured in native-space millimeters using the linked distance between the white and pial surfaces at each of 81,924 cortical points throughout the cortex (25, 27). To improve the ability to compare populations, each subject's cortical thickness map was blurred using a 30-mm surface-based diffusion blurring kernel, chosen to maximize statistical power while minimizing false positives (27). Cortical points were assigned to specific regions using a probabilistic atlas (28). These methods have been validated using both manual measurements (29) and a population simulation (27), and have been used in prior univariate twin studies (2) and studies of normal pediatric brain development (30), among others.

Statistical Analysis. Each subject's measures of cortical thickness were imported into the R statistical environments for structural equation modeling (31). The data were reformatted such that each record represented family-wise (rather than individual-wise) data. The subsequent dataset contained up to eight measures of per individual and up to five individuals per family for each point on the cortical surface. Genetic modeling was performed in OpenMx, a structural equation modeling package fully integrated into the R environment (32).

For each of the 81,924 vertices, genetically informative quadratic latent growth curve models were constructed (33, 34). A simplified path diagram of the model is shown in Fig. 4. A traditional univariate twin model (e.g., the "ACE" model) uses known differences in zygosity to decompose the phenotypic variance into additive genetic (A), shared environmental (C), and unique environmental (E) variance based on differences in observed covariance between family members (35). A nongenetic longitudinal growth curve model uses repeated measures to estimate changes in means and variances with time (36). Compared with other longitudinal methods, latent growth curve models have the advantage that they allow for direct age-based predictions, are robust to missing data cells, and are customizable to unique data structures (37).

The fusion of genetic and longitudinal modeling allows for the simultaneous estimation of changes in variance with time and the decomposition of this variance into genetic and nongenetic factors. Additionally, the inclusion of repeated measures in the quantitative genetic model enables for the separation of measurement error from other sources of environmental

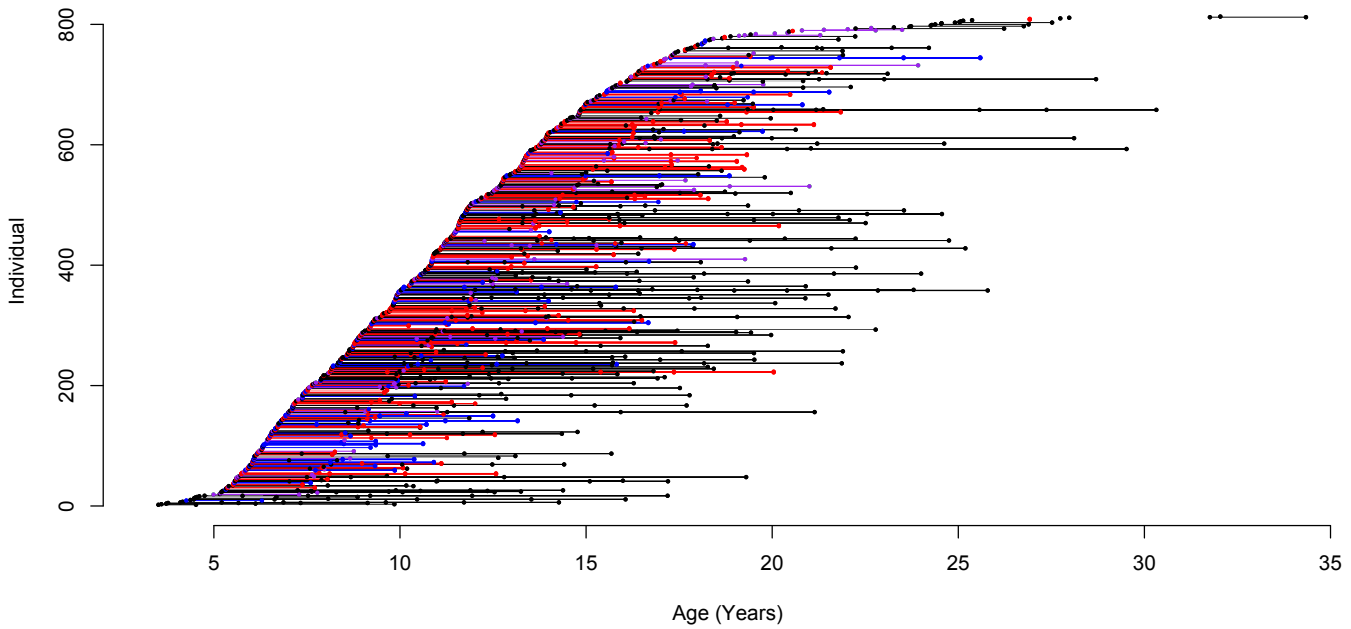

Fig. 3. Age-sorted plot of the sample. Each point represents a single whole-brain MRI, with scans from the same individual linked by lines. Data are color coded by group (red, MZ twins; blue, DZ twins; purple, siblings of twins purple; black, individuals from singleton families).

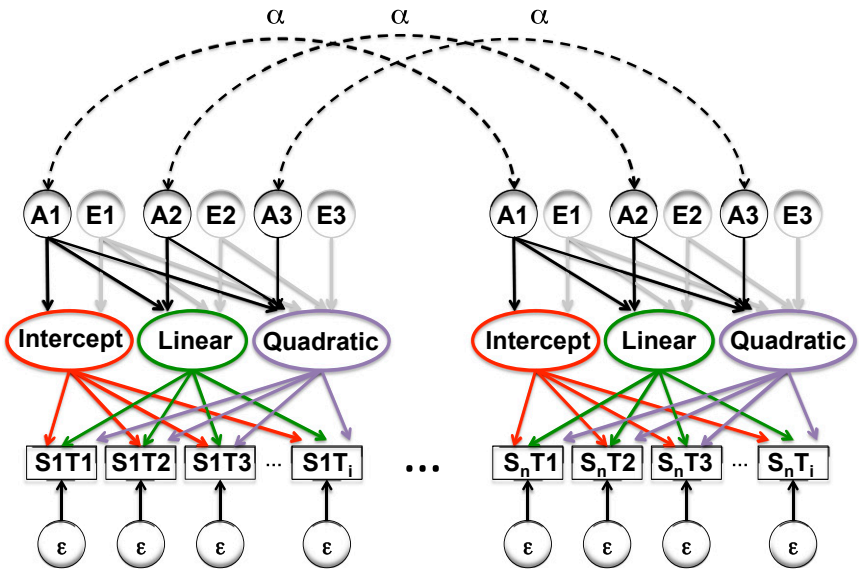

Fig. 4. Simplified path diagram, a graphical representation of the latent growth curve model used in the current study. Rectangles represent the observed measures of cortical thickness of a given vertex *k* for time point *i* from subject *n*. Circles represent additive genetic (A), unique environmental (E), and measurement error (ε) latent factors, all with variance constrained to unity. Double headed (dotted) arrows depict correlations between latent factors, with $\alpha = 1$ for MZ–MZ correlations and $\alpha = 0.5$ for all other cross-sibling correlations. All paths from these factors are freely estimated parameters. Ovals represent the latent growth component of the model. Paths from the intercept path are constrained to unity, paths from the linear latent factor are equal to the scan age at time *i*, and paths from the quadratic factor are equal to the age at time *i* squared. For simplicity, the figure only depicts path coefficients from 2 subjects in a family; in actuality the model included *n* up to 5 and *i* up to 8, for a 40 × 40 covariance matrix of observed measures for each *k*.

variance, resulting in more accurate estimates of heritability than univariate approaches. The rich family structure in the present data made it possibly to use an extended twin design (38, 39), which significantly increases statistical power. Because the study design acquired panel rather than cohort longitudinal data, the age at scan was integrated into the model as a dynamic (e.g., definition) variable to individualize growth curve predictions (40). To increase computational speed, parameters estimating the role of shared environment were excluded from the model based on findings from several prior univariate studies (1, 2). Scripts used to perform these analyses are available online in the *SI Appendix*.

Optimization was performed using maximum likelihood (41). Parameter estimates were used to construct heritability and variance maps at multiple time points, which were projected back onto the cortical surface. To test the statistical significance of changes in variance components with time, submodels were constructed which removed the free parameters modeling change (while maintaining main effects); differences in log likelihood between these models generally follow a χ^2 distribution with degrees of freedom equal to number of parameters removed (35). A submodel in which all genetic effects were removed was also tested. Control of multiple comparisons was performed via false discovery rate (42) using the fdrtool package in R (43). A *q*-value threshold was set at 0.05.

Sex Effects. To quantify potential gene × age × sex interactions, the latent growth curve analysis was repeated at every vertex with a model allowing for scalar sex limitation (44). In this exploratory model, the effects of additive genetic and nongenetic factors on the latent growth parameters were allowed to vary based on the sex of the individual. The statistical significance of these parameters was tested by comparing models with and without the effects of sex limitation. Again, a *q*-value threshold was set at 0.05.

ACKNOWLEDGMENTS. This work was supported by National Institutes of Health Grants MH-20030 and EB-004311.

1. Peper JS, Brouwer RM, Boomsma DI, Kahn RS, Hulshoff Pol HE (2007) Genetic influences on human brain structure: A review of brain imaging studies in twins. *Hum Brain Mapp* 28(6):464–473.
2. Lenroot RK, et al. (2009) Differences in genetic and environmental influences on the human cerebral cortex associated with development during childhood and adolescence. *Hum Brain Mapp* 30(1):163–174.
3. Gogtay N, et al. (2004) Dynamic mapping of human cortical development during childhood through early adulthood. *Proc Natl Acad Sci USA* 101(21):8174–8179.
4. Sowell ER, et al. (2004) Longitudinal mapping of cortical thickness and brain growth in normal children. *J Neurosci* 24(38):8223–8231.
5. van Soelen ILC, et al. (2012) Genetic influences on thinning of the cerebral cortex during development. *Neuroimage* 59(4):3871–3880.
6. Shaw P, et al. (2008) Neurodevelopmental trajectories of the human cerebral cortex. *J Neurosci* 28(14):3586–3594.
7. Gilbert SL, Dobyns WB, Lahn BT (2005) Genetic links between brain development and brain evolution. *Nat Rev Genet* 6(7):581–590.
8. Evans PD, et al. (2005) Microcephalin, a gene regulating brain size, continues to evolve adaptively in humans. *Science* 309(5741):1717–1720.
9. Mekel-Bobrov N, et al. (2005) Ongoing adaptive evolution of ASPM, a brain size determinant in Homo sapiens. *Science* 309(5741):1720–1722.
10. Huttenlocher PR, Dabholkar AS (1997) Regional differences in synaptogenesis in human cerebral cortex. *J Comp Neurol* 387(2):167–178.
11. Colantuoni C, et al. (2011) Temporal dynamics and genetic control of transcription in the human prefrontal cortex. *Nature* 478(7370):519–523.
12. Kang HJ, et al. (2011) Spatio-temporal transcriptome of the human brain. *Nature* 478(7370):483–489.
13. Jones AR, Overly CC, Sunkin SM (2009) The Allen Brain Atlas: 5 years and beyond. *Nat Rev Neurosci* 10(11):821–828.
14. Sommer IEC, Aleman A, Bouma A, Kahn RS (2004) Do women really have more bilateral language representation than men? A meta-analysis of functional imaging studies. *Brain* 127(Pt 8):1845–1852.
15. Luders E, et al. (2006) Gender effects on cortical thickness and the influence of scaling. *Hum Brain Mapp* 27(4):314–324.
16. Sowell ER, et al. (2007) Sex differences in cortical thickness mapped in 176 healthy individuals between 7 and 87 years of age. *Cereb Cortex* 17(7):1550–1560.
17. Peper JS, et al. (2009) Heritability of regional and global brain structure at the onset of puberty: A magnetic resonance imaging study in 9-year-old twin pairs. *Hum Brain Mapp* 30(7):2184–2196.
18. Thompson PM, et al. (2001) Genetic influences on brain structure. *Nat Neurosci* 4(12): 1253–1258.
19. Hollingshead A, Redlich F (1958) *Social Class and Mental Illness: A Community Study* (Wiley, New York).
20. Ad-Dab'bagh Y, et al. (2006) The CIVET image-processing environment: A fully automated comprehensive pipeline for anatomical neuroimaging research. *Proceedings of the 12th Annual Meeting of the Organization for Human Brain Mapping*, ed Corbetta M (Florence, Italy).
21. Collins DL, Neelin P, Peters TM, Evans AC (1994) Automatic 3D intersubject registration of MR volumetric data in standardized Talairach space. *J Comput Assist Tomogr* 18(2):192–205.
22. Sled JG, Zijdenbos AP, Evans AC (1998) A nonparametric method for automatic correction of intensity nonuniformity in MRI data. *IEEE Trans Med Imaging* 17(1):87–97.
23. Zijdenbos AP, Forghani R, Evans AC (2002) Automatic "pipeline" analysis of 3-D MRI data for clinical trials: Application to multiple sclerosis. *IEEE Trans Med Imaging* 21(10):1280–1291.

24. Kim JS, et al. (2005) Automated 3-D extraction and evaluation of the inner and outer cortical surfaces using a Laplacian map and partial volume effect classification. *Neuroimage* 27(1):210–221.
25. MacDonald D, Kabani N, Avis D, Evans AC (2000) Automated 3-D extraction of inner and outer surfaces of cerebral cortex from MRI. *Neuroimage* 12(3):340–356.
26. Robbins S, Evans AC, Collins DL, Whitesides S (2004) Tuning and comparing spatial normalization methods. *Med Image Anal* 8(3):311–323.
27. Lerch JP, Evans AC (2005) Cortical thickness analysis examined through power analysis and a population simulation. *Neuroimage* 24(1):163–173.
28. Collins D, Zijdenbos A, Barre W, Evans A (1999) ANIMAL + INSECT: Improved cortical structure segmentation. *Proceedings of the Annual Conference on Information Processing in Medical Imaging (IPMI)* (Springer, Visegrad, Hungary), pp 210–223.
29. Kabani N, Le Goualher G, MacDonald D, Evans AC (2001) Measurement of cortical thickness using an automated 3-D algorithm: A validation study. *Neuroimage* 13(2): 375–380.
30. Shaw P, et al. (2006) Intellectual ability and cortical development in children and adolescents. *Nature* 440(7084):676–679.
31. R Development Core Team (2006) *R: A Language and Environment for Statistical Computing* (R Foundation for Statistical Computing, Vienna, Austria).
32. Boker S, et al. (2011) OpenMx: An open source extended structural equation modeling framework. *Psychometrika* 76(2):306–317.
33. Neale MC, McArdle JJ (2000) Structured latent growth curves for twin data. *Twin Res* 3(3):165–177.
34. McArdle JJ, et al. (2004) Structural modeling of dynamic changes in memory and brain structure using longitudinal data from the normative aging study. *J Gerontol B Psychol Sci Soc Sci* 59(6):294–304.
35. Neale M, Cardon L (1992) *Methodology for Genetic Studies of Twins and Families* (Kluver, Dordrecht, The Netherlands).
36. Duncan TE, Duncan SC (2004) An introduction to latent growth curve modeling. *Behav Ther* 35:333–363.
37. McArdle JJ, Epstein D (1987) Latent growth curves within developmental structural equation models. *Child Dev* 58(1):110–133.
38. Posthuma D, Boomsma DI (2000) A note on the statistical power in extended twin designs. *Behav Genet* 30(2):147–158.
39. Posthuma D, et al.; Baaré WEC (2000) Multivariate genetic analysis of brain structure in an extended twin design. *Behav Genet* 30(4):311–319.
40. Mehta PD, West SG (2000) Putting the individual back into individual growth curves. *Psychol Methods* 5(1):23–43.
41. Edwards A (1972) *Likelihood: An Account of the Statistical Concept of Likelihood and its Application to Scientific Inference* (University Press, Cambridge, U.K.).
42. Genovese CR, Lazar NA, Nichols T (2002) Thresholding of statistical maps in functional neuroimaging using the false discovery rate. *Neuroimage* 15(4):870–878.
43. Strimmer K (2008) A unified approach to false discovery rate estimation. *BMC Bioinformatics* 9:303.
44. Neale MC, Røysamb E, Jacobson K (2006) Multivariate genetic analysis of sex limitation and G x E interaction. *Twin Res Hum Genet* 9(4):481–489.